Electronic Supplementary Material (ESI) for RSC Advances.

Electronic Supplementary Information

Manipulating the multifunctionalities of polydopamine to prepare high-flux anti-biofouling composite nanofiltration membranes

Runnan Zhang[1,2], Yanlei Su[1,2], Linjie Zhou[1,2], Tiantian Zhou[1,2], Xueting Zhao[1,2], Yafei Li[1,2], Yanan Liu[1,2], Zhongyi Jiang[1,2,*]

[1] *Key Laboratory for Green Chemical Technology of Ministry of Education, School of Chemical Engineering and Technology, Tianjin University, Tianjin 300072, China*

[2] *Collaborative Innovation Center of Chemical Science and Engineering (Tianjin), Tianjin 300072, China*

The characterization of the composite membranes

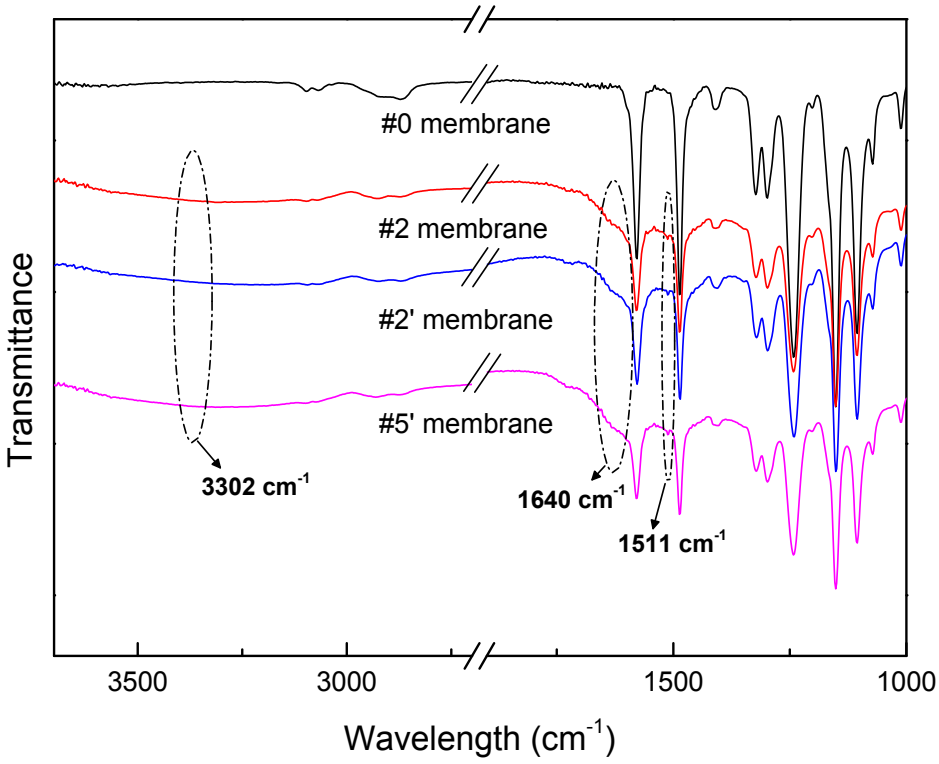

Fig. S1 FTIR spectra of the PES substrate (#0), the PDA/PES composite membrane (#2) and the AgNPs-PDA/PES composite membranes (#2' and #5') and (d) high-resolution Ag3d XPS spectra of the AgNPs-PDA/PES composite membrane (#2').

All three composite membranes, including the PDA/PES composite membrane (#2) and the AgNPs-PDA/PES composite membranes (#2' and #5') exhibited additional peaks at 1511 cm^{-1} and 1640 cm^{-1} compared with the PES substrate (#0), corresponding to the N-H shearing vibrations and the overlap of N-H blending vibrations and C=C resonance vibrations in the aromatic ring, respectively.[1] Moreover, a broad band could also be observed around 3302 cm^{-1}, which ascribed to N-H and O-H stretching vibrations.[2] The new peaks proved the successful modification of PDA on the PES substrate. However, there existed no obvious difference between the spectra of the PDA/PES composite membrane (#2) and the spectra of the AgNPs-PDA/PES composite membranes (#2' and #5').

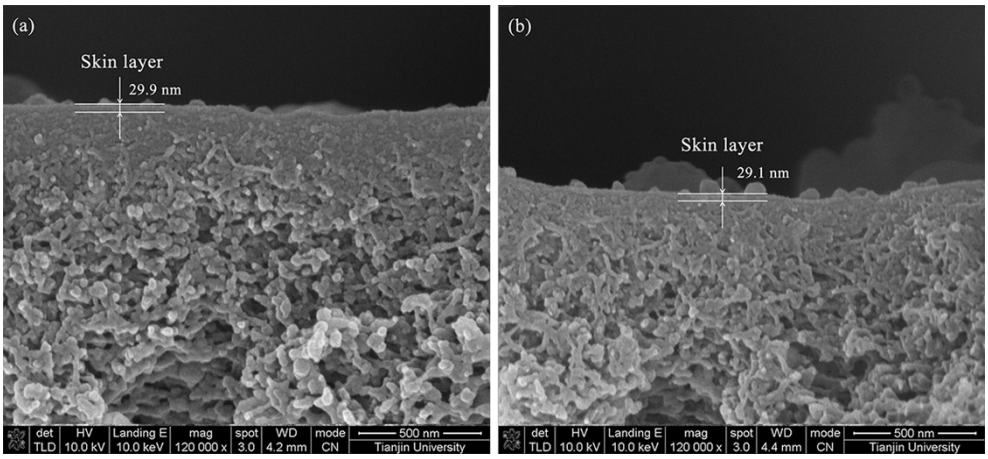

Fig. S2 SEM cross-section images of (a) the PDA/PES composite membrane (2#) and (b) the AgNPs-PDA/PES composite membrane (2'#).

The SEM cross-section images verified the formation of a PDA layer after PDA deposition for 4 h (**Fig. S2(a)**). The thickness of the PDA layer was 29.9 nm, which was in agreement with the data reported by Lee *et al*.[3] After $AgNO_3$ post-treatment, the PDA layer of the AgNPs-PDA/PES composite membrane remained an interconnected structure without obvious defects or decrease in thickness (**Fig. S2(b)**).

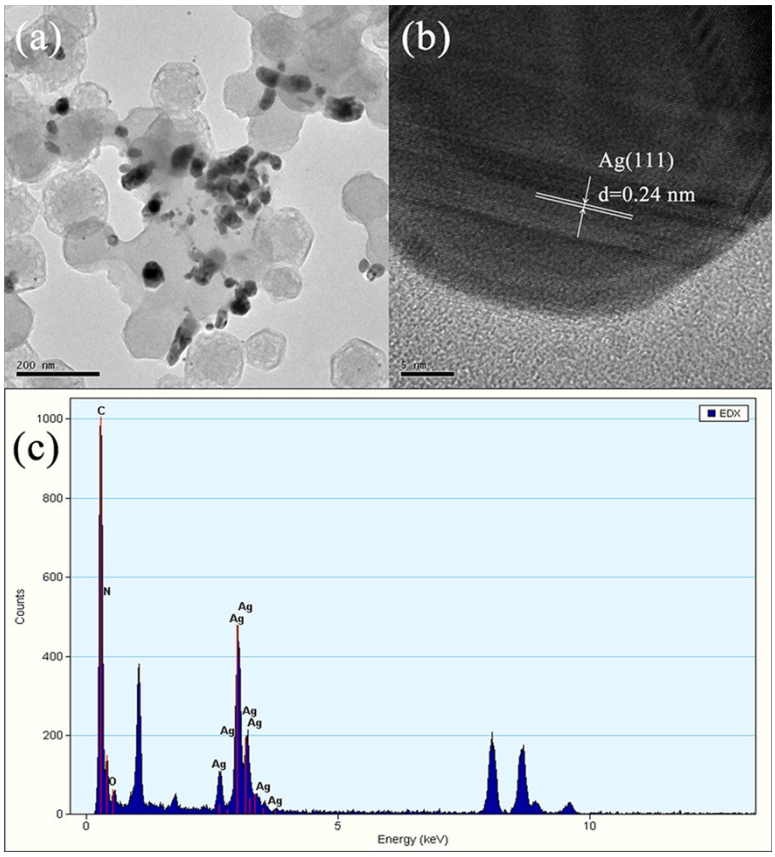

Fig. S3 The characterization of the AgNPs on the composite membrane surface: (a) TEM image of the AgNPs-PDA composite after dissolving the PES substrate; (b) HRTEM image of the AgNPs; (c) EDX results of the AgNPs-PDA composite.

The TEM image showed that the AgNPs exhibited spherical structures (**Fig. S3(a)**), which was coincident with the SEM results. The HRTEM image revealed that the AgNPs possessed a d-spacing value of 0.24 nm (**Fig. S3(b)**), corresponding to the (111) crystalline plane of cubic silver crystal. The EDX results showed intense Ag element signals as well as a relatively weak N element signal (**Fig. S3(c)**), confirming the composition of the AgNPs-PDA composite.

Separation performance of the composite membranes

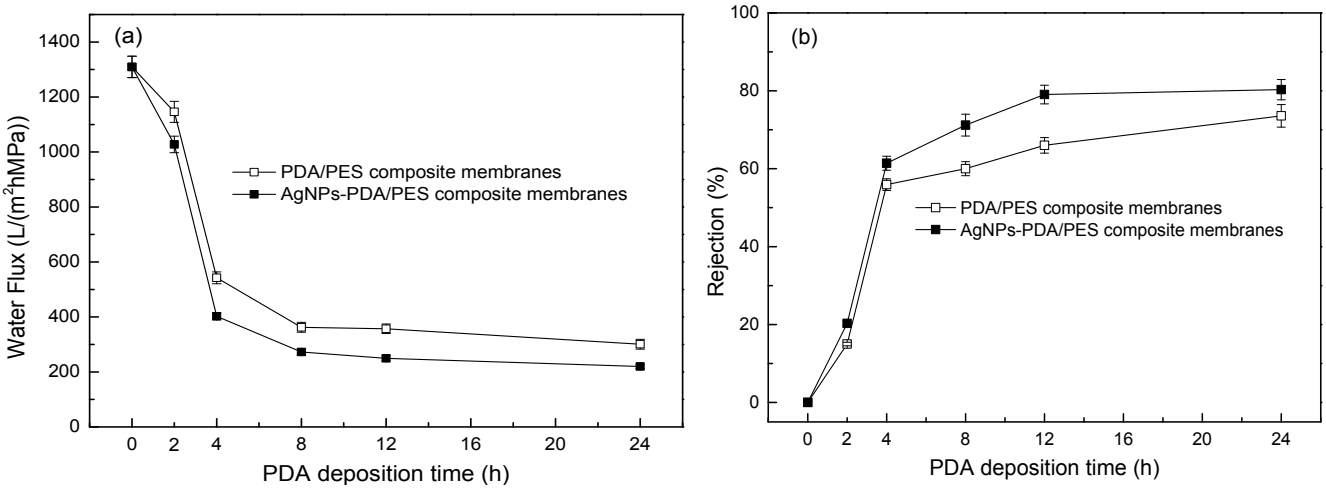

Fig. S4 Effect of PDA deposition time on the separation performance of the PDA/PES and AgNPs-PDA/PES composite membranes: (a) pure water flux, (b) rejection of Orange GII (0.1 g/L). The AgNO3 concentration was fixed at 0 g/Land 1 g/L for PDA/PES and AgNPs-PDA/PES composite membranes, respectively. The AgNO3 treatment time was fixed at 12 h.

As shown in **Fig. S4**, without PDA deposition, the PES substrate (#0) exhibited a pure water flux of 1309.50 L/(m^2hMPa) but nearly zero rejection of Orange GII. This was because the pore size of the PES substrate was about 5-10 nm, which was far larger than the diameters of water molecule as well as hydrolyzed Orange GII molecule. With the increase of PDA deposition time from 2 h to 24 h, the pure water flux of the PDA/PES composite membrane was apparently decreased from 1146.00 to 300.85 L/(m^2hMPa), as illustrated in **Fig. S4(a)**. The flux decline could be explained that within the initial period of time, the deposition of PDA inside the pore as well as on the surface reduced the pore size and led to total blockage of the pores and formation of a PDA layer, which resisted the water pass. Further increase of PDA deposition time would cause the augment of the PDA layer thickness, leading to stronger resistance and hence lower pure water flux. Simultaneously, the rejection was dramatically elevated from 15.00% to 73.57%, as illustrated in **Fig. S4(b)**. On one hand, the further deposition of the PDA oligomers or nanoaggregates might block the nanosized pores of the PDA layer. On the other hand, as time went by,

some residual amine and quinone groups in the PDA oligomers or nanoaggregates might further react and crosslink with each other and get the PDA layer more compact. However, with the deposition time increased from 12 to 24 h, only slight change in flux and rejection could be observed. This was because that with the deposition time prolonged, the increase polymerization degree of PDA could lead to more complex PDA molecules with long molecular chains and disordered structures, which interfered the surface contact and made it more difficult for PDA to adhere to the membrane surface strongly. Accordingly, PDA became less adhesive to the membrane surface and hence caused less change in PDA layer structure[4].

Moreover, although the AgNPs-PDA/PES composite membranes showed a similar variation in performance compared with the PDA/PES composite membranes, they exhibited apparently higher rejections (as high as 79.05% for Orange GII) without sacrificing much pure water flux (**Fig. S4**). Two reasons could be proposed to rationalize this phenomenon. One is that the *in situ* generated AgNPs might block the pores on the PDA layer surface. The other is that silver ions might cause the oxidation of residual catechol groups, facilitating the self-crosslinking of the PDA oligomers or nanoaggregates in the PDA layer. In order to evaluate the impacts of other preparation conditions evidently, PDA deposition time was fixed at 4 h, in which condition the rejection for Orange GII reached a reasonable value of 61.41% with a relatively high pure water flux of 402.50 L/(m^2hMPa).

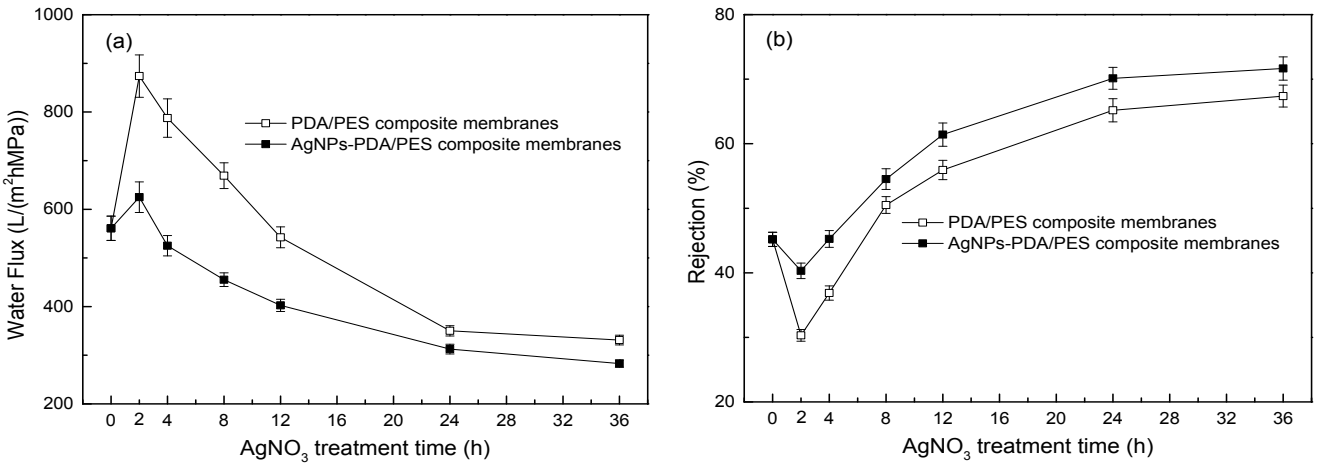

Fig. S5 Effect of $AgNO_3$ treatment time on the separation performance of the PDA/PES and AgNPs-PDA/PES composite membranes: (a) pure water flux, (b) rejection of Orange GII (0.1 g/L). The PDA deposition time was fixed at 4 h. The $AgNO_3$ concentration was fixed at 0 g/Land 1 g/L for PDA/PES and AgNPs-PDA/PES composite membranes, respectively.

As presented in **Fig. S5**, without $AgNO_3$ treatment, the PDA/PES composite membrane (#1) showed a pure water flux of 560.94 L/(m^2hMPa) with the Orange GII rejection of 45.18%. After $AgNO_3$ treatment for 2 h, both the resultant PDA/PES and AgNPs-PDA/PES composite membranes exhibited a sudden increase of the pure water flux with a decrease of Orange GII rejection, simultaneously. This was probably due to the removal of the unstable PDA oligomers or nanoaggregates from the PDA layer by hydrodynamic shearing force. However, with $AgNO_3$ treatment time further rose to 24 h, the pure water flux was decreased down to 350.15 L/(m^2hMPa) for the PDA/PES composite membrane (#6) and 312.60 L/(m^2hMPa) for the AgNPs-PDA/PES composite membrane (#6'), while the Orange GII rejection was increased to 65.18% and 70.13%, respectively. This was presumably because of the further reaction between the residual amine and quinone groups in the PDA layer. After 24 h, the separation performance of the composite membranes remained to be stable. Besides, the higher Orange GII rejections and lower pure water fluxes of the AgNPs-PDA/PES composite membranes, in comparison with those of the PDA/PES composite membranes, were in agreement with the results in **Fig. S4**.

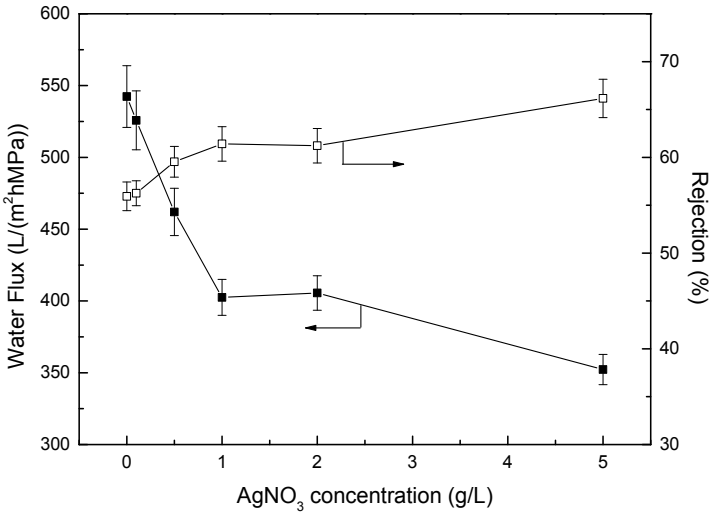

Fig. S6 Effect of $AgNO_3$ concentration on the pure water flux and rejection of Orange GII (0.1 g/L) of the AgNPs-PDA/PES composite membranes. The PDA deposition time and $AgNO_3$ treatment time were fixed at 4 h and 12 h, respectively.

As shown in **Fig. S6**, with the $AgNO_3$ concentration increased from 0 to 5 g/L, the pure water flux was decreased from 542.35 down to 352.25 L/(m^2hMPa), while the rejection of Orange GII was increased from 55.93% up to 66.16%. The reason was that higher $AgNO_3$ concentration would accelerate the oxidation of the catechol groups, leading to the formation of more quinone groups. Therefore, the Micheal addition reaction with amine groups was facilitated, resulting in a more compacted PDA layer. The results further confirmed the impact of AgNPs generation on the PDA layer structure.

Table S1 Comparison of the separation performance of different membranes in the literatures

Membrane name	Dye	Rejection (%)	Flux (L/(m^{2}hMPa))	Operation pressure (MPa)	Ref.
CMCNa/PP	Methyl blue	99.75	8.25	0.8	5
PEI/PAA/PVA/GA	Methyl blue	87.3	8.5	0.5	6
(PEI-modified GO)/PAA/PVA/GA	Congo red	99.5	8.6	0.5	6
PES-TA (M-60)	Methyl green	>99.9	37.2	0.5	7
(NaSS-AC)/PS	Acid red	96	58	0.4	8
PEI-PDA/PES	Methylene blue	96.5	72.5	0.2	1
PSF-PEG	Acid blue	98	76	0.4	9
PVDF-SAN-60	Congo red	97.7	95	0.4	10
PES	Tartrazine	99.5	112.5	1.2	11
$(PSS/PAH)_7$	Glutamine	86.2	132	0.48	12
PES-SPMA	Reactive gyes	>98	145	0.4	13
TA-TMC/PES	Organic GII	99.7	168	0.2	14
PIP-TMC/F127/PES	Alcian blue	95.7	176.2	0.2	15
AgNPs-PDA/PES	Methyl blue	99.64	249.45	0.2	this work
$(ZIF\text{-}8/PSS)_2$/PAN	Methyl blue	98.6	265	0.5	16
Fluorinated PDA/PES	Organic GII	64	461	0.1	17
PVDF/nanoclay/chitosan	Methyl blue	75	500	0.1	18

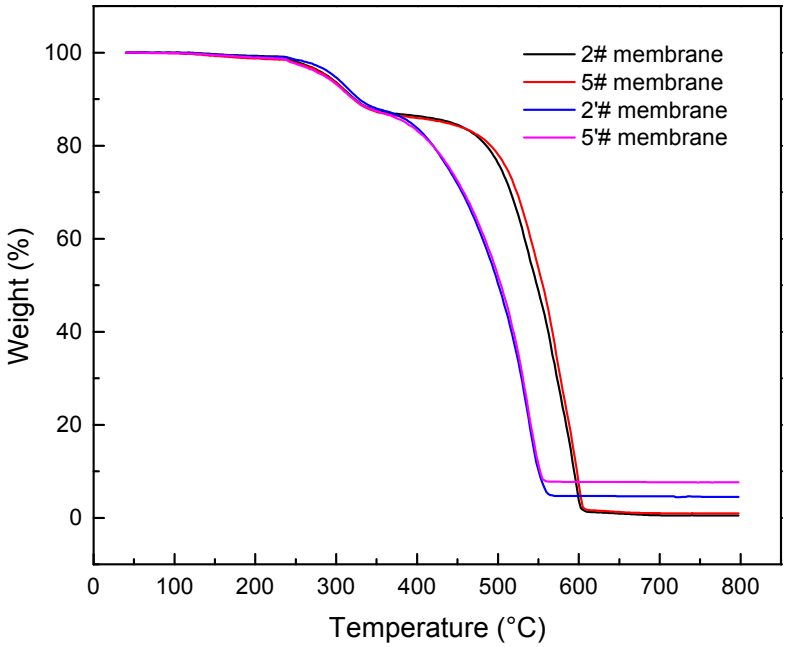

Fig. S7. TGA results of (a) the PES substrate (0#), (b) the PDA/PES composite membrane (2#), (c) the AgNPs-PDA/PES composite membrane (2'#) and (d) the AgNPs-PDA/PES composite membrane (5'#).

Table S2 Total amount of the AgNPs in the composite membranes

Membrane	Residual mass (%)	Mass of AgNPs (%)	Membrane mass (μgcm^{-2})	Total amount of AgNPs (μgcm^{-2})
2#	0.49	-	-	-
5#	0.95	-	-	-
2'#	4.49	4.00	3100	124.00
5'#	7.62	6.67	3200	213.44

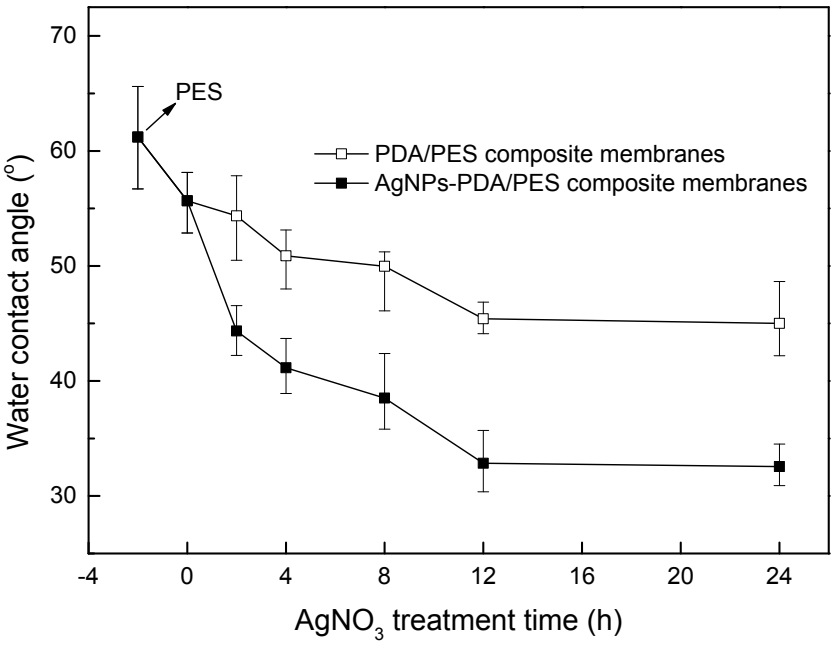

Fig. S8. Static water contact angles of the PDA/PES and AgNPs-PDA/PES composite membranes.

References cited in the Supporting Information:

1. R. Zhang, Y. Su, X. Zhao, Y. Li, J. Zhao and Z. Jiang, *J. Membr. Sci.*, 2014, **470**, 9-17.

2. T. Zhou, L. Luo, S. Hu, S. Wang, R. Zhang, H. Wu, Z. Jiang, B. Wang and J. Yang, *J. Membr. Sci.*, 2015, **489**, 1-10.

3. H. Lee, S. M. Dellatore, W. M. Miller and P. B. Messersmith, *Science*, 2007, **318**, 426-430.

4. D. Chai, Z. Xie, Y. Wang, L. Liu and Y. J. Yum, *ACS Appl. Mater. Interfaces*, 2014, **6**, 17974-17984.

5. S. Yu, Z. Chen, Q. Cheng, Z. Lü, M. Liu, C. Gao, *Sep. Purif. Technol.*, 2012, **88**, 121-129.

6. N. Wang, S. Ji, G. Zhang, J. Li, L. Wang, *Chem. Eng. J.*, 2012, **213**, 318-329.

7. Q. Zhang, H. Wang, S. Zhang, L. Dai, *J. Membr. Sci.*, 2011, **375**, 191-197.

8. A. Akbari, S. Desclaux, J. C. Rouch, P. Aptel, J. C. Remigy, *J. Membr. Sci.*, 2006, **286**, 342-350.

9. M. Amini, M. Arami, N. M. Mahmoodi, A. Akbari, *Desalination.* 2011, **267**, 107-113.

10. H. P. Srivastava, G. Arthanareeswaran, N. Anantharaman, V. M. Starov, *Desalination*, 2011, **282**, 87-94.

11. C. Aydiner, Y. Kaya, Z. Beril Gönder, I. Vergili, *J. Chem. Technol. Biotechnol.*, 2010, **85**, 1229-1240.

12. S. U. Hong, M. L. Bruening, *J. Membr. Sci.*, 2006, **280**, 1-5.

13. A. V. R. Reddy, J. J. Trivedi, C. V. Devmurari, D. J. Mohan, P. Singh, A. P. Rao, S. V. Joshi, P. K. Ghosh, *Desalination*, 2005, **183**, 301-306.

14. Y. Zhang, Y. Su, J. Peng, X. Zhao, J. Liu, J. Zhao, Z. Jiang, *J. Membr. Sci.*, 2013, **429**, 235-242.

15. Y. Zhang, Y. Su, W. Chen, J. Peng, Y. Dong, Z. Jiang, H. Liu, *J. Membr. Sci.*, 2011, **382**, 300-307.

16. R. Zhang, S. Ji, N. Wang, L. Wang, G. Zhang, J. R. Li, *Angew. Chem. Int. Ed. Engl.*, 2014, **53**, 9775-9.

17. Y. Li, Y. Su, X. Zhao, X. He, R. Zhang, J. Zhao, X. Fan, Z. Jiang, *ACS Appl. Mater. Interfaces*, 2014,

6, 5548-57.

18. P. Daraei, S. S. Madaeni, E. Salehi, N. Ghaemi, H. S. Ghari, M. A. Khadivi, E. Rostami, *J. Membr. Sci.*, 2013, **436**, 97-108.